

Theoretical basis for the corrosion inhibition feature of Argan oil

G. Gece

Department of Chemistry, Faculty of Natural Sciences, Architecture and Engineering, Bursa Technical University, Bursa, 16310 Turkey

Received April 3, 2017; Accepted May 2, 2017

Natural oils play a pivotal role in corrosion inhibition of various metals and alloys. However, their potential inhibition efficiency in acidic media has been barely investigated from a theoretical point of view. Despite a shared experimental justification, the corrosion inhibition feature of such oils resulted in a sustained debate on how the inhibition mechanism could be related to their ingredients. Given the need to better understand the protection behaviour of Argan oil on carbon steel in molar HCl solutions, the electronic properties of two unsaturated fatty acids, i.e., oleic and linoleic acids were studied by density functional theory (DFT) calculations. The protonated forms of oleic and linoleic acids yielded quantum chemical parameters that confirm linoleic acid to be the most stable unsaturated fatty acid, which seems to be responsible for the inhibition efficiency of Argan oil in acidic medium.

Keywords: Argan oil; Oleic acid; Linoleic acid; Corrosion inhibition; DFT.

INTRODUCTION

Despite its relatively limited corrosion resistance, carbon steel is more commonly used than any other metal, and has long been admired for its versatility and low cost. Generally, the application of corrosion inhibitors is one of the most common practices for the protection of steel structures and their alloys in industry [1]. In many cases, the role of inhibitors is to form a surface coating one or several molecular layers thick that serves as a barrier. This in turn depends on the chemical composition, the structure of the inhibitor, the nature of the metal surface, and the properties of the medium. Structural and electronic parameters such as type of the functional group, steric, and electronic effects, are broadly responsible for the inhibition efficiency of any inhibitor, that is, for the adsorption mechanism [2].

Environmental awareness has been gaining attention in recent years, along with growing emphasis on substitution of harmful inhibitors with effective non-hazardous alternatives [3]. Considerable success has been achieved in this regard through the use of some natural oils for corrosion inhibition of different metals [4].

A recent study by Afia *et al.* [5] found evidence that in the presence of Argan oil the corrosion of C38 steel in chloride solution was considerably slowed. Argan oil, obtained from the pit of *Argania spinosa*, is a vegetable oil rich in unsaturated fatty acids (~80%) mainly oleic and linoleic acids (46-48 and 31-35%, respectively) [6]. The experimental results showed that the inhibition efficiency of Argan oil reached about 85% at a concentration of 5 g/L. A

tentative explanation was offered that this inhibition effect may be due to physical adsorption resulting from the displacement of adsorbed water molecules by the inhibitor species, leading to specific adsorption on the metal surface.

It is clear that an evaluation of the protection property of Argan oil from a theoretical point of view would be needed before more definite conclusions about the underlying inhibition mechanism could be drawn. The present study, prompted by the successful application of theoretical calculations in corrosion inhibitor research [7-13], is offered as a further contribution to gain a better understanding of the inhibition effect of Argan oil, whose underlying mechanism is still far from explicit.

COMPUTATIONAL DETAILS

All quantum mechanical geometry optimizations and single-point energy computations were achieved using the Gaussian 09 package [14]. Geometries of all investigated systems were optimized at the density functional theory level using the 6-311G+(d,p) basis set and B3LYP functional. The bulk solvent effects were included through the Integral Equation Formalism version of the Polarizable Continuum Model (IEF-PCM). For the calculations of the interaction energies between oleic and linoleic acids and iron surface, two models were built based on the X-ray diffraction structures [15]. Each of them contained three individual oleic or linoleic acid molecules oriented vertically on the surface in lengthwise direction. A moderate spacing of 10Å was inserted between these molecules which was seen to be sufficient to allow packing. The

* To whom all correspondence should be sent:
E-mail: gokhangc@gmail.com

carboxylic oxygen atoms lie 3 Å above the Fe (110) surface. The Fe10 cluster with a lattice constant of 2.86 Å for body-centered-cubic Fe was used to represent the Fe(110) surface [16]. Single-point energy calculations were performed by using universal force field approach with the semiempirical quantum mechanical (QM/PM6) method to calculate the interaction energy due to the compromise between available computing power and the attempt to study the system as thoroughly as possible [17].

RESULTS AND DISCUSSION

Fatty acids are organic acids characterized by the presence of a carboxyl group at one end and a methyl group at the other end. Due to their variation in length and degree of saturation, they are classified either as saturated or unsaturated. The saturated ones are straight-chains and consist of a carbon chain with single bonds, while the unsaturated ones contain one or more double carbon-carbon bonds (C=C), which introduces fixed bends into the carbon chain. The results of gas chromatography analysis of Argan oil [5] revealed that the oil tested as corrosion inhibitor contained large amounts of unsaturated fatty acids. The most abundant was the mono-unsaturated oleic acid (45.1%) and the bi-unsaturated linoleic acid (34.5%). This is the gist of why our theoretical calculations particularly focus on those two molecules. As can be seen from Fig. 1, oleic acid, a C-18 fatty acid, consists of a long chain of carbon atoms with a central C=C bond introducing a slight kink and a monocarboxyl head. On the other hand, linoleic acid is an 18-carbon unsaturated fatty acid with two double bonds in positions 9 and 12, respectively, and both are in the *cis* configuration.

Evidence from earlier electrochemical measurements propounds that the monolayer characteristics of fatty acids are strictly dependent upon pH change [18]. At low pH (< 7), oleic acid is principally protonated and no added ion-dipole interaction exists between the ionized and unionized groups; at intermediate pHs (7-9) almost half of the acid groups are protonated; at high pHs (>9) oleic acid is mostly ionized, and ionic repulsion between the carboxylate ions keeps the molecules apart [19]. The experimental data resorted to were predicated on the results of electrochemical tests in 1 M HCl solution, and therefore, a rough-and-ready way to examine whether the criterion of protonation is satisfied here was to run DFT calculations for the protonated forms of these compounds (Fig. 1).

Thus, to validate whether the calculation method selected fulfils the requirements of accuracy for

geometry optimization, one would need to compare experimental geometric parameters with the theoretical predictions. We will focus particularly on the geometry of oleic acid (Fig. 1(a)) for which experimental data are available. Below its freezing point (13.3°C), three oleic acid solid state polymorphs (α , β , and γ) have been identified [20].

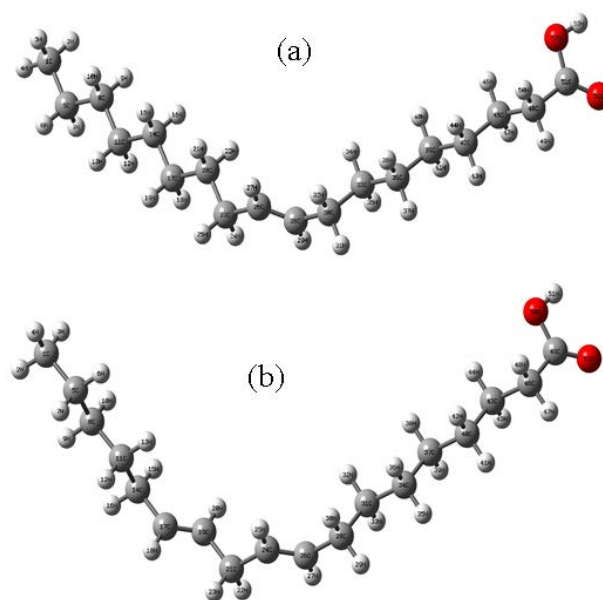


Fig. 1. Optimized structures using the B3LYP/6-311+G(d,p) level for the protonated forms of (a) oleic acid and (b) linoleic acid in the gas phase.

The β phase is unique in contrast to the α and γ phases due to its presence only in oleic acid and appears as two forms: stable β_1 and metastable β_2 . Guided by known structures for the stable β_1 phase, configurations for two crystallographically different molecules, A and B were considered [21]. Some selected bond lengths, bond angles, and torsion angles of molecules A and B were compared with those calculated for oleic acid. Bond distances are largely unremarkable: C-C single and double-bond distances are virtually identical at *ca.* 1.51 Å and 1.31 Å, respectively. In addition, the C51-O52 single bonds and C51=O54 double bonds are also very similar for the structures. The carbon-carbon bonds between C20 and C1 show slight contractions from 1.533 Å to 1.509 (molecule A) and 1.502 Å (molecule B). This trend, although not pronounced, is likely a consequence of reduced steric interactions due to the increase in dihedral angles. There are no other obvious trends noted except for nearly uniformly larger bond distances for the optimized structure. However, this corresponds to only about 0.06 Å at its maximum and is not considered to be very significant. Also, the predicted oleic acid structure agrees rather closely with the experimentally determined conformations, given

that the calculated results are for a single isolated molecule. The sum of the angles around the carboxylic carbon atom C₅₁ does not differ much from planarity, and particularly for dihedral angles between adjacent chain atoms C₂₃–C₁, very close agreement with experimental data was obtained (differences are less than 1°). Larger difference was obtained for the carboxylic acid moiety. This indicates that the positions of C₅₁, O₅₂ and O₅₄ atoms are rather affected by the molecular packing. In general, the bond distances and angles obtained from the X-ray structure determinations compare favorably with those determined from the calculations, and can provide a starting point to calculate other parameters, such as the energies of the frontier molecular orbitals.

The chemical bond between the inhibitor and the surface can be considered a combination of double interactions of the highest occupied molecular orbitals (HOMO) and the lowest unoccupied molecular orbitals (LUMO). Certain quantum chemical parameters, i.e., frontier orbital energies such as E_{HOMO} , E_{LUMO} , and $\Delta E = E_{\text{LUMO}} - E_{\text{HOMO}}$, were used for the sake of comparison in Table 1. According to the results, the highest E_{HOMO} (-6.639 eV), the lowest E_{LUMO} (-0.309 eV) and ΔE (6.330 eV) values are found for linoleic acid. The results for E_{HOMO} , E_{LUMO} and ΔE yield that linoleic acid molecule could prevail for the inhibitory action of Argan oil as a constituent, compared to oleic acid. These results were also supported by the global reactivity parameters. In Table 1, global properties obtained by the frontier molecular orbital energies according to Koopmans theorem [22] are also listed. The ionization potential (I) and electron affinity (A)

are given by $I = -E_{\text{HOMO}}$ and $A = -E_{\text{LUMO}}$. In numerical applications, chemical potential μ and hardness η are expressed on the basis of finite difference approximations in terms of the ionization potential I and the electron affinity A ; $-\mu = \frac{1}{2}(I + A) = \chi$ and $\eta = \frac{1}{2}(I - A)$, where μ is the chemical potential and χ is the electronegativity. The electrophilicity is a descriptor of reactivity that allows a quantitative classification of the global electrophilic nature of a molecule within a relative scale and is effectively the power of a system to soak up electrons. The electrophilicity index ω can be expressed by $\omega = \mu^2/2\eta$ and the global softness is defined as $\sigma = 1/\eta$.

During the interaction of the inhibitor molecule with bulk metal, electrons flow from the lower electronegative molecule to the higher electronegative metal until the chemical potential becomes equalized. The fraction of the transferred electron, ΔN , was estimated according to Pearson [24], $\Delta N = \chi_m - \chi_i / 2(\eta_m + \eta_i)$, where the indices m and i refer to metal atom and inhibitor molecule, respectively. The fraction of transferred electrons given in the table is calculated for iron metal, the experimental work function of polycrystalline Fe (4.5 eV) [25] was employed for electronegativity, and a global hardness of zero was used due to the $I = A$ approximation for bulk iron. If $\Delta N < 3.6$, the inhibition efficiency increases by increasing the electron-donating ability of these molecules to donate electrons to the metal surface [7]. Linoleic acid has the largest fraction of transferred electrons to the iron metal, closely followed by oleic acid, in agreement with the above ordering supported by electronic parameters.

Table 1. Calculated quantum chemical descriptors at the B3LYP/6-311G+(d,p) basis set for oleic and linoleic acids in gas and aqueous phases.

Compound	Oleic acid		Linoleic acid	
	G	A	G	A
Phase ^a				
E_{HOMO} (eV)	-6.714	-6.726	-6.639	-6.676
E_{LUMO} (eV)	-0.303	-0.422	-0.309	-0.421
ΔE ($E_{\text{L}} - E_{\text{H}}$) (eV)	6.411	6.304	6.330	6.255
μ (D)	2.064	2.507 (2.47/2.63±0.05) ^b	2.072	2.529
ω	1.920	2.026	1.907	2.013
χ	3.509	3.574	3.474	3.549
η	3.206	3.152	3.165	3.128
σ	0.312	0.317	0.316	0.319
ΔN	0.155	0.147	0.162	0.152
E_{T}	-0.802	-0.788	-0.791	-0.782

^aG – gas phase ($\epsilon = 1.0$), A – aqueous phase ($\epsilon = 78.5$); ^b Ref. [26]

The dipole moment of oleic acid in the gaseous phase is not known, and as experimental moments only the calculated dipole moments were available for these molecules on the basis of Debye's and Kirkwood-Fröhlich's theories [26]. The fit of the calculated dipole moments with the experimental dipole moments is also of the same accuracy, considering the values for aqueous phase. The dipole moment of linoleic acid is found to be slightly higher than that of oleic acid, which probably increases its adsorption on the metal surface.

To understand the adsorption of Argan oil over an iron surface at a molecular level, two models were used for single-point energy calculations. For ease of presentation, each model was composed of two-directional oleic or linoleic acid molecules and two ranks of Fe clusters labeled OA, LA, F1, and F2, in which OA and LA represent individual oleic and linoleic acid molecules, and F1 and F2 represent the two ranks of Fe clusters (Fig. 2). To investigate the interactions between the iron clusters in the model, F1F2 and OAOA (or LALA) were considered to be two independent entities. The interaction energy (E) between the two ranks of iron clusters and the OA molecules (Model 1) can be expressed as follows:

$$E(\text{Model 1}) = E(\text{OAF1F2OA}) - E(\text{F1F2}) - E(\text{OAOA}) \quad (1)$$

A similar equation can be written to express the interaction energy (E) between the two ranks of iron clusters and the LA molecules (Model 2):

$$E(\text{Model 2}) = E(\text{LAF1F2LA}) - E(\text{F1F2}) - E(\text{LALA}) \quad (2)$$

According to the results derived from the calculations by the PM6 method, interaction energies were found to be $-5846.41 \text{ kcal mol}^{-1}$ and $-115.35 \text{ kcal mol}^{-1}$ for Models 1 and 2, respectively. The results indicate that the interaction energy for Model 2 is dominated by the main interaction between Fe and O atoms of linoleic acid molecules due to the hybridization. However, it should be noted here that structural and energetic factors cannot always be in direct correlation for a metal atom- π interaction because the strength of the interaction is grossly decided by the electrostatic interactions and the size of the π -system. Our calculated results indicate a preference for linoleic acid to be oriented towards the metal surface, and the hydrophobic component to be oriented away from the surface. In the light of the findings above, linoleic acid appears to be the predominant molecule which synergistically interacts with other active substances naturally present in the oil and enables Argan oil to be an effective corrosion inhibitor in acidic media.

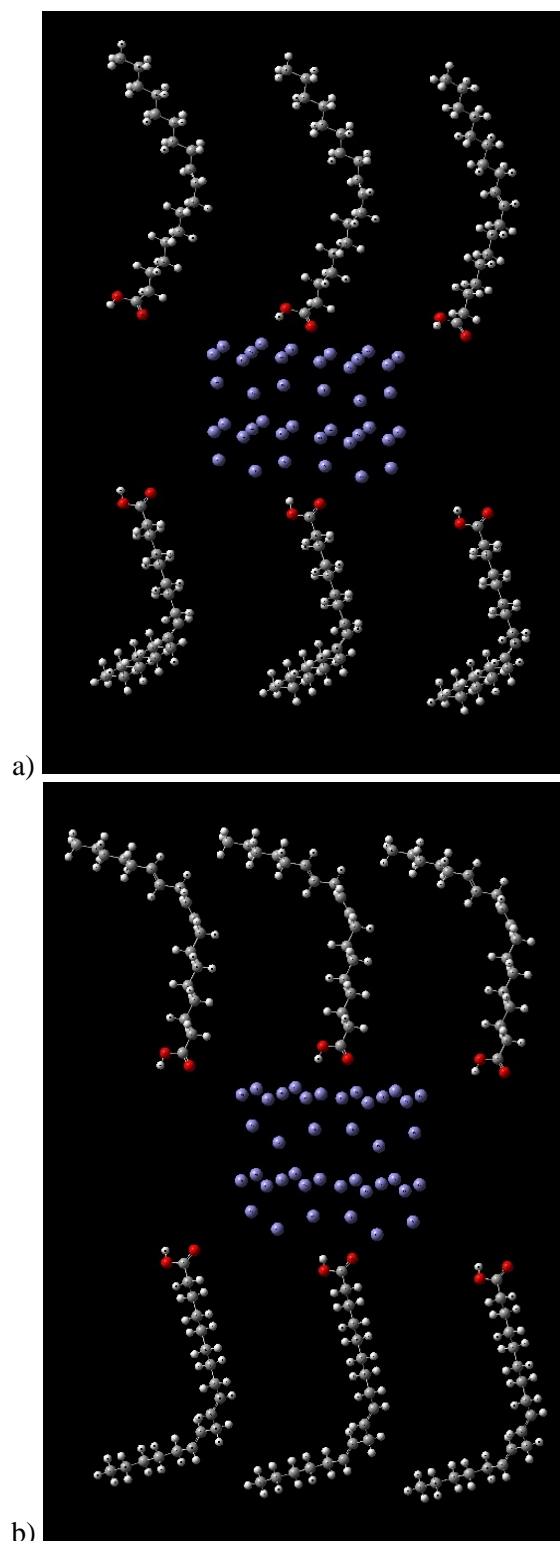


Fig. 2. Regularly spaced iron clusters (purple spheres) trapped in (a) Model 1 between OA molecules and (b) Model 2 between LA molecules.

CONCLUSIONS

Despite the vast literature on natural oils as corrosion inhibitors there was no unified explanation for all known examples. We have shown how an understanding of typical inhibition efficiency of such oils can arise from the use of density functional

theory calculations. Although a clear decomposition of the energetic contributions of individual interactions is, strictly speaking, impossible, approximate propensities can be derived. Noteworthy is the fact that the ground state of the protonated forms of the compounds yields the electronic and global reactivity parameters giving considerable credence for the identified structures in acidic medium. On the basis of the data obtained at the B3LYP/6-311+G(d,p) level, we can confirm that the most stable unsaturated fatty acid is linoleic acid, which seems to be responsible for the inhibition efficiency of Argan oil in chloride solutions.

REFERENCES

1. K. K. Anupama, K. Ramya, A. Joseph, *Measurement*, **95**, 297 (2017).
2. K. Cherrak, A. Dafali, A. Elyoussfi, Y. El Ouadi, N. K. Sebbar, M. El Azzouzi, H. Elmsellem, E. M. Essassi, A. Zarrouk, *JMES*, **8**, 636 (2017).
3. G. Gece, *Corros. Sci.*, **53**, 3873 (2011).
4. M. A. Dar, *Ind. Lubr. Tribol.*, **63**, 227 (2011).
5. L. Afia, R. Salghi, L. Bammou, E. Bazzi, B. Hammouti, L. Bazzi, A. Bouyanzer, *J. Saudi Chem. Soc.*, **18**, 19 (2014).
6. Z. Charrouf, D. Guillaume, *Eur. J. Lipid Sci. Technol.*, **110**, 632 (2008).
7. G. Gece, *Corros. Sci.*, **50**, 2981 (2008).
8. I. B. Obot, S. A. Umoren, Z. M. Gasem, R. Suleiman, B. El Ali, *J. Ind. Eng. Chem.*, **21**, 1328 (2015).
9. H. M. Abd El-Lateef, *Corros. Sci.*, **92**, 104 (2015).
10. G. Gece, *Corros. Rev.*, **33**, 195 (2015).
11. M. K. Awad, M. R. Mustafa, M. M. Abouelnga, *Prot. Met. Phys. Chem. Surf.*, **52**, 156 (2016).
12. A. Valbon, M. A. Neves, A. Echevarria, *Int. J. Electrochem. Sci.*, **12**, 3072 (2017).
13. M. E. Mashuga, L. O. Olasunkanmi, E. E. Ebenso, *J. Mol. Struct.*, **1136**, 127 (2017).
14. M. J. Frisch, G. W. Trucks, H. B. Schlegel, G. E. Scuseria, M. A. Robb, J. R. Cheeseman, G. Scalmani, V. Barone, B. Mennucci, G. A. Petersson, H. Nakatsuji, M. Caricato, X. Li, H. P. Hratchian, A. F. Izmaylov, J. Bloino, G. Zheng, J. L. Sonnenberg, M. Hada, M. Ehara, K. Toyota, R. Fukuda, J. Hasegawa, M. Ishida, T. Nakajima, Y. Honda, O. Kitao, H. Nakai, T. Vreven, J. A. Montgomery, Jr., J. E. Peralta, F. Ogliaro, M. Bearpark, J. J. Heyd, E. Brothers, K. N. Kudin, V. N. Staroverov, R. Kobayashi, J. Normand, K. Raghavachari, A. Rendell, J. C. Burant, S. S. Iyengar, J. Tomasi, M. Cossi, N. Rega, J. M. Millam, M. Klene, J. E. Knox, J. B. Cross, V. Bakken, C. Adamo, J. Jaramillo, R. Gomperts, R. E. Stratmann, O. Yazyev, A. J. Austin, R. Cammi, C. Pomelli, J. W. Ochterski, R. L. Martin, K. Morokuma, V. G. Zakrzewski, G. A. Voth, P. Salvador, J. J. Dannenberg, S. Dapprich, A. D. Daniels, Ö. Farkas, J. B. Foresman, J. V. Ortiz, J. Cioslowski, D. J. Fox, Gaussian 09, Revision C.01, Gaussian, Inc., Wallingford CT, 2010.
15. M. Iwahashi, Y. Kasahara, H. Matsuzawa, K. Yagi, K. Nomura, H. Terauchi, Y. Ozaki, M. Suzuki, *J. Phys. Chem. B*, **104**, 6186 (2000).
16. G. E. Doan, *The Principles of Physical Metallurgy*, McGraw-Hill, New York, 1953.
17. J. J. P. Stewart, *J. Mol. Model.*, **13**, 1173 (2007).
18. J. H. Schulman, A. H. Hughes, *Proc. R. Soc. London A*, **138**, 430 (1932).
19. J. R. Kanicky, D. O. Shah, *J. Colloid Interface Sci.*, **256**, 201 (2002).
20. M. Suzuki, T. Ogaki, K. Sato, *J. Am. Oil Chem. Soc.*, **62**, 1600 (1985).
21. F. Kaneko, K. Yamazaki, K. Kitagawa, T. Kikyo, M. Kobayashi, *J. Phys. Chem. B*, **101**, 1803 (1997).
22. T. Koopmans, *Physica*, **1**, 104 (1934).
23. B. Gómez, N. V. Likhanova, M. A. Dominguez-Aguilar, R. Martínez-Palou, A. Vela, J. L. Gazquez, *J. Phys. Chem. B*, **110**, 8928 (2006).
24. R. G. Pearson, *Inorg. Chem.*, **27**, 734 (1988).
25. H. Michaelson, *J. Appl. Phys.*, **48**, 4729 (1977).
26. F. F. De Sousa, S. G. C. Moreira, S. J. Dos Santos Da Silva, J. D. Nero, Jr. P. Alcantara, *J. Bionosci.*, **3**, 139 (2009).

ТЕОРЕТИЧНА ОСНОВА ЗА ХАРАКТЕРИСТИКАТА НА ИНХИБИРАНЕ НА КОРОЗИЯТА НА АРГАНОВО МАСЛО

Г. Гедже

Департамент по химия, Факултет по природни науки, архитектура и инженерство, Технически университет на Бурса, Бурса, 16310 Турция

Получена на 3 април, 2017 г.; коригирана на 2 май, 2016 г.

(Резюме)

Естествените масла играят централна роля при инхибиране на корозията на различни метали и сплави. Въпреки това, потенциалната им ефективност на инхибиране в киселинни среди е много слабо изследвана от теоретична гледна точка. Въпреки частичното експериментално потвърждение, характеристиката за инхибиране на корозията на такива масла води до продължителен дебат за това как механизмът на инхибиране може да бъде свързан с техните съставки. Предвид необходимостта от по-добро разбиране на поведението на защитата на аргановото масло върху въглеродната стомана в моларни разтвори на HCl, електронните свойства на две ненаситени мастни киселини, т.е. молекули на олеинова и линоленова киселина, са изследвани чрез изчисления с теория на функционалната плътност (DFT). Протонираните форми на олеиновите и линоленовите киселини дадоха квантови химични параметри, които потвърждават, че линоленовата киселина е най-стабилната ненаситена мастна киселина, която също изглежда е отговорна за ефективността на инхибиране на арганово масло в кисела среда.